

1 **Quantitative analysis of chest computed tomography of COVID-19 pneumonia using a software**
2 **widely used in Japan**

3

4 Minako Suzuki^{1*}, Yoshimi Fujii^{2¶}, Yurie Nishimura^{2¶}, Kazuma Yasui^{2¶}, Hidefumi Fujisawa^{1¶}

5

6 ¹ Department of Radiology, Showa University Northern Yokohama Hospital, Yokohama, Kanagawa,

7 Japan

8 ² Department of Radiology, Fujisawa City Hospital, Fujisawa, Kanagawa, Japan

9

10 * Corresponding author:

11 E-mail: minacom69@gmail.com (MS)

12

13 **Short title:** Quantitative analysis of chest CT of COVID-19 pneumonia

14

15 [¶]These authors contributed equally to this work.

16

17 **Abstract**

18 This study aimed to determine the optimal conditions to measure the percentage of area
19 considered as pneumonia (pneumonia volume ratio, PVR) and the computed tomography
20 (CT) score due to coronavirus disease 2019 (COVID-19) using the Ziostation2 image
21 analysis software (Z2; Ziosoft, Tokyo, Japan), which is popular in Japan, and to evaluate its
22 usefulness in assessing the clinical severity. We included 53 patients (41 men and 12 women,
23 mean age: 61.3 years) diagnosed with COVID-19 using the polymerase chain reaction who
24 had undergone chest CT and were hospitalized between January 2020 and January 2021.
25 Based on the COVID-19 infection severity, the patients were classified as mild (n=38) or
26 severe (n=15). For 10 randomly selected samples, the PVR and CT scores by Z2 under
27 different conditions and the visual simple PVR and CT scores were compared, and the
28 conditions with the highest statistical agreement were determined. The usefulness of the
29 clinical severity assessment based on PVR and CT scores using Z2 under the determined
30 conditions was statistically evaluated. The best agreement with the visual measurement was
31 achieved by the Z2 measurement condition of ≥ -600 HU. The areas under the receiver
32 operating characteristic curves, the Youden index, and the sensitivity, specificity, and p-values
33 of PVR and CT scores by Z2 were as follows: PVR; 0.881, 18.69, 66.7, 94.7, and <0.001 , CT
34 score; 0.77, 7.5, 40, 74, and 0.002, respectively. We determined the optimal condition for
35 assessing the PVR of COVID-19 pneumonia using Z2 and demonstrated that the AUC of
36 PVR was higher than that of the CT score in the assessment of clinical severity. The
37 introduction of new technologies is time-consuming and expensive; our method has high
38 clinical utility and can be promptly used in any facility where Z2 has been introduced.

39 40 **Introduction**

41 The coronavirus disease 2019 (COVID-19) pandemic caused by the novel coronavirus severe
42 acute respiratory syndrome coronavirus 2 (SARS-CoV-2) was first identified in Wuhan,
43 China, and reported in December 2019 [1]. The pandemic prevails with an increasing number
44 of infections and deaths. In Japan, the first COVID-19 case was reported in January 2020 [2],
45 and by April 2023, over 33 million people had been infected, and more than 74000 people
46 had died [3]. After the Omicron strain of SARS-CoV-2 became prevalent, the number of
47 severe cases complicated by pneumonia decreased, and the vaccination had spread socially.
48 In May 2023, the legal classification was changed, and it was decided that a COVID-19
49 infection would be treated on the same level as an influenza virus infection [3].

50 This study was conducted with the aim of determining how the radiology department
51 of a city hospital in Japan could use existing image analysis software to contribute to clinical
52 practice at a time when the pre-Delta strain COVID-19 virus was predominant.

53 During the study period, COVID-19 infection had a high complication rate with
54 pneumonia, especially in older adults [4, 5], with a high rate of aggravation and mortality,
55 and it became necessary to distribute limited medical resources. The discrimination between
56 mild and severe cases at the emergency department was an important and burdensome task.
57 Typically, the severity was determined by symptoms, age, complications, blood tests, and
58 computed tomography (CT) findings. The CT findings were generally evaluated visually, and
59 the CT scores based on visual evaluation were not accurate or objective and took time and
60 effort on the part of the evaluator. There are many reports on the CT severity assessment of
61 COVID-19-associated pneumonia using an imaging software. The measurement methods and
62 evaluation conditions differ for each individual tool, and few of them have been widely
63 adopted in clinical settings.

64 The Ziostation2 image analysis software (Z2; Ziosoft, Tokyo, Japan) had been
65 introduced in approximately 300 facilities in Japan, which was designed to quantify

66 pulmonary emphysema in patients with chronic obstructive pulmonary disease. When a
67 region above a certain concentration is recognized as a pneumonia region, the pneumonia
68 volume ratio (PVR) can be measured by changing the threshold setting of the CT value (Fig
69 1a, b). To the best of our knowledge, there are no reports of COVID-19 pneumonia
70 assessment by Z2.

71

72 **Fig 1. Images displayed on the console of the Z2.** Z2 monitor screen. The PVR above a
73 certain concentration is displayed in the upper right corner (red square). LAV, low attenuation
74 volume; LL, left lower lobe; LU, left upper lobe; nLAV, not LAV (lung volume other than
75 LAV); PVR, pneumonia volume ratio; RL, right lower lobe; RM, right middle lobe; RU, right
76 upper lobe; Z2, Ziostation2.

77

78 Since Z2 has not been set to evaluate pneumonia, it is necessary to determine the
79 threshold in Hounsfield units (HUs) for it. Therefore, it was decided to set the threshold at the
80 concentration that most closely matched the visual evaluation.

81 In this study, we determined the appropriate conditions for the evaluation of
82 COVID-19 pneumonia by Z2 through comparison with visual evaluation results and
83 examined the usefulness of the clinical severity assessment of Z2.

84

85 **Materials and Methods**

86 **Study population**

87 This study adhered to the principles of the Declaration of Helsinki and was approved by the
88 Ethical Review Committee of Fujisawa City Hospital (approval number: F2021022). The

89 study was conducted retrospectively using imaging data and electronic medical records. An
90 informed consent was provided by all patients in an opt-out manner on the website.

91 We evaluated patients diagnosed with COVID-19 using a polymerase chain reaction
92 test who required a chest CT scan at our hospital and inpatient hospital care between January
93 2020 and January 2021. The patients who had an initial CT scan at another hospital or those
94 who were initially treated at another hospital and subsequently transferred to our hospital, and
95 cases without pneumonia findings on chest CT were excluded. Ten samples were randomly
96 selected from patients under 65 years of age and with an uncomplicated condition.

97 The clinical severity of COVID-19 was classified as mild ($\text{SpO}_2 > 93\%$) or severe
98 ($\text{SpO}_2 \leq 93\%$, intubation, and intensive care unit management) based on the symptoms at the
99 time of hospitalization, according to the guidelines of the Ministry of Health and Welfare [4].
100 The clinical severity, symptoms, comorbidities, blood test values, and clinical course were
101 retrieved from the electronic medical records.

102

103 **CT protocol**

104 The chest CT scans were obtained using 64-multidetector CT scanners (SOMATOM
105 Definition AS 64; Siemens Healthineers, Erlangen, Germany). The CT parameters used at
106 our hospital were as follows: 120 kVp, 160-316 mA current intelligent control (auto mA),
107 and 5 mm slice thickness reconstruction. All CT examinations were performed without the
108 use of intravenous contrast agents. The EV Report picture archiving and communication
109 system (PACS) (PSP Corporation, Tokyo, Japan) was used to evaluate the CT findings.

110

111 **CT image analysis**

112 Two radiologists evaluated the CT findings of pneumonia in all patients (Y.N. and M.S.) in
113 consultation for the presence or absence of ground-glass opacity (GGO) (-/+), crazy-paving
114 finding (-/+), consolidation (none/mild/moderate/severe), and emphysema (-/+).

115 For the 10 selected participants, visual evaluation of the PVR was performed independently
116 by two radiologists (Y.F. and M.S.) using the free-form curve drawing tool of the PACS by
117 adding up the area of the lungs and the pneumonia area freehand at 1.5-cm intervals in the
118 coronal chest CT images (Fig 2). In the same participants, the two radiologists independently
119 scored the percentage of pneumonia area in each lobe using visual measurements (0: 0%, 1:
120 25%, 2: 25–50%, 3: 50–75%, and 4: 75–100%).

121

122 **Fig 2. Visual measurement of PVR.** Two radiologists independently selected the entire lung
123 field and pneumonia area every 1.5 cm on the coronal view using a drawing tool on the PACS
124 (PSP Corporation, Tokyo, Japan), and added these up to measure the PVR. The blue line
125 indicates the entire lung field (mm²), and the yellow line indicates the pneumonia area (mm²).
126 The minimum and maximum in the figure represent CT values in the region. PACS, report
127 picture archiving and communication system; PVR, pneumonia volume ratio; min, minimum;
128 max, maximum; SD, standard deviation.

129

130 Z2 provided the quantification of the emphysema, healthy lung parenchyma, GGO,
131 and consolidation based on a HU. Z2 can divide segments and calculate total volumes for
132 both the right and left lungs. In the measurement of PVR and CT scores in the 10 selected
133 participants using Z2, the lung fields above a particular concentration were set as pneumonia
134 areas and measured at ≥ -500 HU, ≥ -550 HU, ≥ -600 HU, ≥ -650 HU, and ≥ -700 HU. Z2
135 may not recognize the subpleural consolidation area as a lung field, and the total lung volume

136 may be underestimated (Fig 3); therefore, radiologist A (M.S.) made the appropriate
137 corrections manually.

138

139 **Fig 3. Dorsal subpleural consolidations are not recognized as part of the lung and**
140 **require manual correction.** The white arrows indicate the areas that needed to be manually
141 corrected.

142

143 **Statistical analysis**

144 The presence of significant differences in participant background (age, sex, number of days
145 from disease onset to CT evaluation, and laboratory test results) between the mild and severe
146 groups was evaluated using the t-test and chi-square test. The accuracy between the gross
147 measurements of PVR and CT scores by two independent radiologists and the measurements
148 by Z2 were evaluated using the Spearman's rank correlation coefficient. The influence of
149 possible confounding factors of participant background (age, sex, number of days from
150 disease onset to CT evaluation, and presence of comorbidities) on the severity classification
151 of PVR by Z2 was evaluated using the bivariable logistic regression. The usefulness of PVR
152 and CT scores by Z2 under the determined conditions, primary laboratory tests, and CT
153 findings in the clinical severity assessment was determined by the receiver operating
154 characteristic (ROC) curves, Youden index, sensitivity, specificity, and p-values. All
155 statistical analyses were performed using the SPSS software (version 27; IBM, Armonk, NY,
156 USA).

157

158 **Results**

159 The number of patients diagnosed with COVID-19 using a polymerase chain reaction test
160 who required a chest CT scan at our hospital and inpatient hospital care between January
161 2020 and January 2021 were 91. Of these, three patients who received initial treatment at
162 another hospital and 28 patients who had no findings of pneumonia on chest CT were
163 excluded. Two cases were excluded from the study because the thin slice data necessary for
164 Z2 measurement were not saved, and five cases could not be measured by Z2 for unknown
165 reasons.

166 **Fig 4. The flow chart shows the process of determining the number of study cases to 53.**

167
168 In total, 53 participants (41 men and 12 women, with a median age of 61.3 years; 38 in the
169 mild group and 15 in the severe group) were included. Table 1 shows the participants'
170 demographics (age, sex, and presence of comorbidities), laboratory findings, and CT findings.
171 Fifty-two participants presented with COVID-19 symptoms; however, there was no
172 significant difference in the severity of the symptoms between the mild and severe disease
173 groups. Significant differences in the number of days from disease onset to CT evaluation
174 and the presence of comorbidities were found between the two groups. In addition, laboratory
175 results revealed that C-reactive protein (CRP) and lactate dehydrogenase (LDH) levels
176 differed significantly between the two groups. The CT findings showed a significant
177 difference in consolidation between the two groups.

178

179 **Table 1. Patient background, blood test, and CT findings**

Factor	Total (n = 53)	Mild (n = 38)	Severe (n = 15)	p-value
--------	----------------	---------------	-----------------	---------

Age (years; median)	61.28 (66)	58.95 (59.5)	67.2 (67.00)	0.148
Sex (male; %)	41 (77.4)	27 (71.1)	14 (93.3)	0.081
Date from onset to CT (range)	6.0 (1–14)	5.2 (1–12)	7.9 (4–14)	0.016
Comorbidities ^a (%)	18 (34.0)	9 (23.7)	9 (60.0)	0.012
DM (%)	6 (11.3)	3 (7.9)	3 (20.0)	0.21
COPD (%)	5 (9.4)	2 (5.3)	3 (20.0)	0.098
CRF (%)	4 (7.5)	3 (7.9)	1 (6.7)	0.879
Obesity (%)	6 (11.3)	1 (2.6)	5 (33.3)	0.0015
Malignancy (%)	3 (5.7)	1 (2.6)	2 (13.3)	0.129
Symptoms (any)	52 (98.1)	37 (97.4)	15 (100)	0.526
Fever (%)	46 (86.8)	33 (86.8)	13 (86.7)	0.986
Cough (%)	22 (41.5)	14 (36.8)	8 (53.3)	0.272
Taste disorder (%)	7 (16.2)	7 (18.4)	0 (0)	0.074
Vomiting or diarrhea (%)	9 (17.0)	8 (21.1)	1 (6.7)	0.21
<hr/>				
Blood tests (range)				
WBC ($\times 10^9/L$)	6.6 (2.5–21.7)	6.3 (2.5–21.7)	7.2 (3.5–12.3)	0.33
Lymphocytes (%)	17.8 (4–46.5)	11.6 (4–46.5)	7.5 (5.2–26.4)	0.085
CRP (mg/dL)	8.1 (0.02–29.6)	2.9 (0.02–29.6)	13.1 (2.4–26.0)	0.005
LDH (U/L)	364.8 (144–1136)	302.8 (144–834)	521.8 (233–1136)	< 0.001
AST (U/L)	50.2 (14–160)	46.3 (14–160)	60.1 (25–131)	0.213
ALT (U/L)	43.5 (7–200)	39.97 (7–200)	52.27 (15–163)	0.308
Creatinine (mg/dL)	1.39 (0.31–14.9)	1.15	0.998 (0.52–2.34)	0.455

	(0.31–14.9)			
eGFR (mL/min)	65.8 (30–144)	65.4 (1.6–144)	66.93 (22–100)	0.853
CT findings				
GGO (+) (%)	53 (100)	38 (100)	15 (100)	1
Crazy paving (+) (%)	8 (15.1)	5 (13.2)	3 (20.0)	0.53
Consolidation (–)				
(%)	23 (43.4)	21 (55.3)	2 (13.3)	
(+) (%)	17 (32.1)	12 (31.6)	5 (33.3)	
(++) (%)	8 (15.1)	5 (13.2)	3 (20.0)	
(+++)	5 (9.4)	0 (0)	5 (33.3)	0.0006
Z2 (≥ -600 HU)				
PVR mean (median, range)	12.44 (1.63–63.26)	7.59 (1.63–40.11)	24.71 (3.32–63.26)	< 0.001
CT score mean (median, range)	6.62 (8, 5–15)	5.87 (5, 5–11)	8.53 (7, 5–15)	< 0.001

180

181 CT: computed tomography, DM: diabetes mellitus, COPD: chronic obstructive pulmonary
 182 disease, CRF: chronic renal failure, WBC: white blood cell, CRP: C-reactive protein, LDH:
 183 lactate dehydrogenase, AST: aspartate aminotransferase, ALT: alanine aminotransferase,
 184 eGFR: estimated glomerular filtration rate, GGO: ground-glass opacity, Z2: Ziostation2,
 185 PVR: pneumonia volume ratio

186 ^aComorbidities were defined as presence of any of the following: DM, COPD, severe
 187 cardiovascular disease, severe CRF, obesity, malignancy under treatment,
 188 immunosuppression, and liver cirrhosis.

189

190 Table 2 shows the results of the Spearman’s correlation between Z2 (under each
 191 condition; PVR: ≥ -500 HU, ≥ -550 HU, ≥ -600 HU, ≥ -650 HU, and ≥ -700 HU, CT score:
 192 ≥ -500 HU, and ≥ -600 HU) and the two radiologists for PVR and the CT scores in the 10
 193 participants without comorbidities, respectively. While the accuracy between the two
 194 radiologists and Z2 for PVR was equally high at ≥ -500 HU to ≥ -600 HU, the accuracy for
 195 CT scores was higher at ≥ -600 HU than at ≥ -500 HU. Based on these results, the Z2
 196 measurement condition for COVID-19 pneumonia that achieved the best accuracy with the
 197 gross measurement was determined to be ≥ -600 HU.

198

199 **Table 2. Results of the Spearman’s test of PVR and CT score by two radiologists and**
 200 **Ziostation2 of five/two conditions in the 10 selected patients**

		Reader	≥ -500	≥ -550	≥ -600	≥ -650	≥ -700
		B	HU	HU	HU	HU	HU
Reader A	PVR	0.879	0.976	0.976	0.976	0.964	0.818
	CT score	0.976	0.639		0.651		
Reader B	PVR		0.842	0.842	0.842	0.83	0.661
	CT score		0.584		0.696		

201

202 PVR: pneumonia volume ratio, CT: computed tomography,

203 Reader A: M.S., Reader B: Y.F.

204

205 Figs 4 and 5 show the ROC curves and boxplots corresponding to the classification
206 of disease severity by PVR and CT score using Z2 (≥ -600 HU), CRP, and LDH. The areas
207 under the curve (AUCs) were 0.881, 0.77, 0.788, and 0.842, respectively.

208

209 **Fig 5. ROC curves for PVR, CT score, CRP, and LDH.** ROC curve for **a.** PVR using Z2 (\geq
210 -600 HU) and **b.** CT scores using Z2 (≥ -600 HU), **c.** CRP, and **d.** LDH. ROC, receiver
211 operating characteristic; PVR, pneumonia volume ratio; Z2, Ziostation2; CT, computed
212 tomography; CRP, C-reactive protein; LDH, lactate dehydrogenase; SD, standard deviation

213

214 **Fig 6. Boxplots of PVR, CT score, and CRP.** Boxplots for **a.** PVR using Z2 (≥ -600 HU), **b.**
215 CT scores using Z2 (≥ -600 HU), **c.** CRP, and **d.** LDH. 1: mild group, 2: severe group. Error
216 bars indicate outliers. PVR, pneumonia volume ratio; CT, computed tomography; Z2,
217 Ziostation2; CRP, C-reactive protein; LDH, lactate dehydrogenase

218

219 The Youden index values for PVR and CT scores at ≥ -600 HU by Z2, CRP, and
220 LDH were 18.69, 7.5, 5.26, and 306.5, respectively. The sensitivities for PVR and CT scores
221 at ≥ -600 HU by Z2 were 66.7% and 40%, respectively. The specificities for PVR and CT
222 scores at ≥ -600 HU by Z2 were 94.7% and 74%, respectively. The p-value for PVR at \geq
223 -600 HU by Z2 was $p < 0.001$, and that for CT scores at ≥ -600 HU by Z2 was $p = 0.002$
224 (Table 3). The bivariable logistic regression of PVR (≥ -600 HU) according to age, sex, date
225 from onset to CT, and comorbidities showed no significant effects, except for comorbidities
226 (Table 4). The sensitivity and specificity were 66.7% and 89.5% when the PVR threshold
227 was 18, and 60% and 97.4% when the PVR threshold was 20, respectively.

228

229 **Table 3. Cut-off values for pneumonia volume ratio and blood test to differentiate mild**
 230 **and severe groups**

	Youden index	AUC	Sensitivity	Specificity	Lower 95% CI	Upper 95% CI	p-value
PVR (≥ -600 HU)	18.69	0.881	66.7	94.7	0.781	0.981	< 0.001
CT score (≥ -600 HU)	7.5	0.77	40	74	0.629	0.911	0.002
CRP	5.26	0.788	86.7	68.4	0.664	0.912	< 0.001
LDH	306.5	0.842	86.7	68.4	0.729	0.956	< 0.001

231

232 AUC: area under the curve, PVR: pneumonia volume ratio, CT: computed tomography, CRP:
 233 C-reactive protein, LDH: lactate dehydrogenase, CI: confidence interval

234

235 **Table 4. Bivariable logistic regression of PVR (≥ -600 HU) according to age, sex, number**
 236 **of days from onset to CT, and comorbidities**

237

Predictor	OR (95% CI)	p-value
PVR (≥ -600 HU)	1.131 (1.048–1.221)	0.002
Age	1.031 (0.979–1.086)	0.246
PVR (≥ -600 HU)	1.124 (1.049–1.206)	0.001
Sex	0.000 (0.146–1530.796)	0.252

PVR (≥ -600 HU)	1.126 (1.044–1.214)	0.002
Number of days from onset to CT	1.058 (0.837–1.339)	0.637
PVR (≥ -600 HU)	1.137 (1.045–1.237)	0.003
Comorbidities (any)	9.795 (1.432–67.002)	0.02

238

239 PVR, pneumonia volume ratio; OR, odds ratio; CT, computed tomography; CI, confidence
240 interval

241

242 The evaluation of PVR and CT scores in patients affected by COVID-19-associated
243 pneumonia by Z2 was highly consistent with the visual-evaluation results under the condition
244 of ≥ -600 HU. The AUC and Youden index of the ROC curve by Z2 (≥ -600 HU) were 0.881
245 and 18.69 for PVR, and 0.77 and 7.5 for the CT score, respectively, indicating that they are
246 useful for clinical severity classification.

247

248 Discussion

249 The chest CT plays a major role in COVID-19 treatment, including severity judgment and
250 prognostic prediction. In clinical practice and in previous studies, the spatial progression of
251 pneumonia on CT has been evaluated with naked eye, and the accuracy and homogeneity
252 have not been ensured.

253 In this study, we examined the usefulness of determining the severity of
254 COVID-19-associated pneumonia using Z2, an image analysis software widely available in

255 Japan. This methodology can be easily deployed at facilities that have Z2 and thus has high
256 clinical utility.

257 Several reports evaluated the percentage of lesion area of COVID-19-associated pneumonia
258 in each lobe of the lung visually and scored them to determine the disease severity [6-10].
259 Yang et al. [6] visually classified the percentage of lesion area in each segment as 0%, <50%,
260 and >50%. Li et al. [7] reported that the percentage of lesion area in each lobe was visually
261 classified as 0%, 0–25%, 25–50%, 50–75%, and 75–100%, and scored on a scale of 0–20.
262 The authors found that the optimal threshold for the severe group was 7.5. Francone et al. [9]
263 used a similar classification, with a mortality risk cut-off of 18. Li et al. [8] also reported
264 scores of 0:0%, 1:<5%, 2:5–25%, 3:25–50%, 4:50–75%, and 5:>75% or higher, with a
265 cut-off score of 7, a sensitivity of 80%, and a specificity of 82.8% for the severely ill group.
266 The cut-off value for clinical severity classification by CT score varies depending on the
267 method and on how the severity is classified.

268 The CT scores based on visual evaluations that do not require special software or techniques
269 are widely used in clinical settings. This type of evaluation is subjective; however, it has been
270 reported that the inter-evaluator difference is small, and the results of this study are in
271 agreement. However, the score measurement for each lobe in 25–50% increments is
272 troublesome and imposes a burden on the emergency unit staff. Inoue et al. [11] reported that
273 three visual CT score evaluations required 25.7-41.7 s, 27.7-39.5 s, and 48.9-80.0 s,
274 respectively. Novel methods for the quantitative and automated measurement of the spatial
275 progression of COVID-19-associated pneumonia have been reported since the early days of
276 the pandemic [12-21].

277 Using the commercially available image analysis software, Timaran-Montenegro et al. [12]
278 automatically classified –700 to –1000 HU as normal lung, and –500 to 20 HU as pneumonia
279 regions, and compared the survival vs non-survival groups. The percentage of normal lung

280 was a significant independent factor according to a multinomial logistic analysis. Colombi
281 et al. [13] defined the region of -950 to -700 HU as well as aerated lungs and reported that
282 the measurement by commercially available software and visual measurement were very
283 similar and useful for severity evaluation. In the 10 cases selected in our study, the
284 correlation between the automated measurement by Z2 under the condition of ≥ -600 HU and
285 the macroscopic measurement was high: very high for PVR (correlation coefficient
286 $0.842-0.976$) and moderate for the CT score (correlation coefficient $0.651-0.696$).
287 As there were no previous reports of using Z2 as a tool to evaluate diseases such as
288 pneumonia with increased lung concentration, the concentration range for pneumonia was
289 determined to be ≥ -600 HU in this study, based on the high degree of consistency in terms of
290 visual PVR and CT score.

291 The range of normal lung, GGO, and consolidation reported in each study using software
292 varied as follows: between: -1000 to -600 HU for normal lung, -750 to -100 HU for GGO,
293 and -399 to -69 HU for consolidation [10-15]. Many previous studies set the lower limit of
294 the GGO range at -800 to -700 HU; however, -600 HU was selected as the lower limit in
295 this study due to the high degree of agreement with the visual findings. This was probably
296 because it is difficult to recognize a faint increase in concentration based on visual evaluation
297 compared to the software-assisted evaluation. It is an advantage of the software-assisted
298 evaluation that it can detect faint concentrations; however, considering that the CT evaluation
299 of COVID-19-associated pneumonia is generally based on visual evaluation, the detection of
300 faint concentrations that are not measurable by visual evaluation leads to clinical
301 discrepancies.

302 Grassi et al. [14] reported that the percentage of normal lung, emphysema, and consolidation
303 measured by three different software tools were inconsistent. Granata et al. [15] compared the
304 results obtained from two different software tools and reported that the correlation between

305 them was not high enough. The algorithms in which each software is based are different, and
306 therefore comparisons cannot be made under uniform conditions. Z2 is a software tool owned
307 by more than 300 facilities in Japan. Therefore, an assessment method based on the use of Z2
308 may be immediately available at these facilities and have a high clinical significance. In
309 addition, the introduction of new technologies is time-consuming and expensive.

310 Okuma et al. [17] reported that the CT score and the percentage of opacity (PVR in this
311 study) obtained using commercially available AI-based software showed a similar AUC;
312 however, in this study the AUC corresponding to PVR and the CT score estimated by Z2
313 under ≥ -600 HU was higher in the case of PVR. Theoretically, the CT scoring method can
314 differ by up to 24% in one lobe at the same point, making it less accurate than PVR. When
315 automated measurement of the same standard becomes widespread, the evaluation by PVR is
316 likely to replace CT scores.

317 Recently, there have been many reports on the diagnosis and severity assessment of
318 COVID-19-associated pneumonia using AI [16-20]. In a study on COVID-19-associated
319 pneumonia using an AI-based software developed by Ziosoft, the company that developed Z2,
320 Aoki et al. [20] measured the CT lesion extent separately for normal lung, GGO, reticulation,
321 and consolidation. In this study, the pneumonia area was evaluated by combining GGO and
322 consolidation; however, more accurate qualitative and quantitative evaluation will be possible
323 if AI-based software is adopted for this purpose in the future.

324 In this study, Z2 sometimes misidentified subpleural consolidation as extrapulmonary,
325 requiring manual correction. Inoue et al. [11] reported the measurement errors with the use of
326 U-NET due to the inclusion of atelectasis, fibrosis, and air trapping in the density mask.
327 When a software tool is used, the measurement is carried out automatically; however, the
328 error checking may still need to be performed by human staff.

329 In this study, we showed the optimal conditions for measuring the PVR and
330 CT score in cases of COVID-19-associated pneumonia using Z2, a widely used image
331 analysis software in Japan, and provided a guideline for clinical severity evaluation based on
332 it. Therefore, defining a Z2-based assessment method has a high clinical significance, and
333 replacing visual evaluation with existing image analysis software represents a way to quickly
334 reduce the burden on clinicians at each facility.

335 Binomial logistic regression analysis showed no significant effects of age, sex, or
336 time from onset to CT on PVR.

337 In terms of CT findings, consolidation was significantly higher among the severe
338 group, in agreement with previous reports [9, 19-21]. Several laboratory tests have been
339 reported to be indicators of COVID-19 infection. In our study, both CRP and LDH were
340 significant items, again in agreement with previous reports [22, 23].

341 The major limitation of this study was the small number of participants at a single
342 facility. The other limitations were that the manual correction of the subpleural consolidation
343 in the Z2 measurement was performed by a single radiologist and the significance of
344 inter-operator differences was not evaluated. Moreover, PVR assumed the area of ≥ -600 HU
345 to be a surrogate value for COVID-19 pneumonia, but no histological confirmation was
346 available. The PVR measurements were uniformly performed regardless of the background
347 lesions affecting emphysema, fibrosis, or atelectasis.

348 In conclusion, we determined the optimal conditions that best approximates visual
349 evaluation for assessing COVID-19-associated pneumonia using Z2, one of the most popular
350 image analysis software tools in Japan and demonstrated that the AUC of PVR was higher
351 than that of CT score in the assessment of clinical severity. The introduction of new
352 technologies is time-consuming and expensive; this method has high clinical utility and can
353 be adopted immediately in any facility where Z2 is available for use.

354

355 **Acknowledgments**

356 We would like to thank Dr. Noriko Hida and Dr. Eisuke Inoue for their guidance on the
357 statistical analysis, and Ms. Hokazono and Editage (www.editage.com) for English language
358 editing. We also appreciate the support from our proofreaders and editors. In addition, we are
359 grateful to the clinicians at Fujisawa City Hospital for their insightful advice.

360

361

362

363

364

365

366

367

368

369

370

371

372

373

374

375

376 **References**

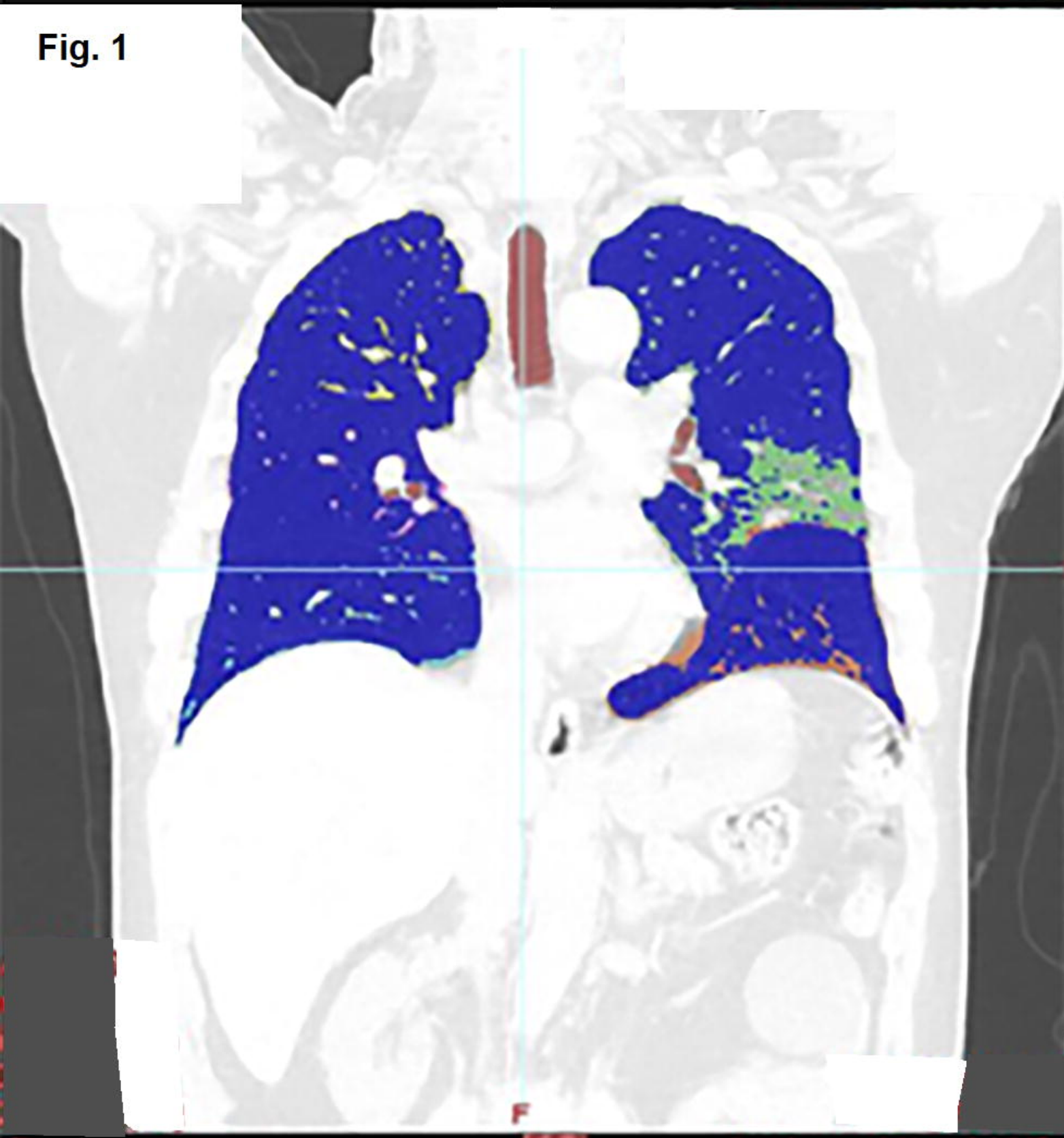
- 377 1. Hui DS, Azhar EI, Madani TA, Ntoumi F, Kock R, Dar O, et al. The continuing
378 2019-nCoV epidemic threat of novel coronaviruses to global health—The latest 2019
379 novel coronavirus outbreak in Wuhan, China. *Int J Infect Dis.* 2020;91: 264-266. doi:
380 10.1016/j.ijid.2020.01.009.
- 381 2. Furuse Y, Ko YK, Saito M, Shobugawa Y, Jindai K, Saito T, et al. Epidemiology of
382 COVID-19 outbreak in Japan, from January-March 2020. *Jpn J Infect Dis.* 2020;73:
383 391-393. doi: [10.7883/yoken.JJID.2020.271](https://doi.org/10.7883/yoken.JJID.2020.271).
- 384 3. Japanese Ministry of Health, Labour and Welfare. Regarding the response after the
385 transition to Category 5 infectious diseases of the new coronavirus infectious disease;
386 2023. Available from: <https://www.mhlw.go.jp/stf/corona5rui.html>.
- 387 4. Japanese Ministry of Health, Labour and Welfare. COVID-19 in Japan. Available from:
388 <https://covid19.mhlw.go.jp/extensions/public/index.html> (2022).
- 389 5. Matsunaga N, Hayakawa K, Terada M, Ohtsu H, Asai Y, Tsuzuki S, et al. Clinical
390 epidemiology of hospitalized patients with coronavirus disease 2019 (COVID-19) in
391 Japan: report of the COVID-19 Registry Japan. *Clin Infect Dis.* 2021;73: e3677-e3689.
392 doi: [10.1093/cid/ciaa1470](https://doi.org/10.1093/cid/ciaa1470).
- 393 6. Yang R, Li X, Liu H, Zhen Y, Zhang X, Xiong Q, et al. Chest CT severity score: an
394 imaging tool for assessing severe COVID-19. *Radiol Cardiothorac Imaging.* 2020;2:
395 e200047. doi: [10.1148/ryct.2020200047](https://doi.org/10.1148/ryct.2020200047).

- 396 7. Li K, Fang Y, Li W, Pan C, Qin P, Zhong Y, et al. CT image visual quantitative evaluation
397 and clinical classification of coronavirus disease (COVID-19). *Eur Radiol.* 2020;30:
398 4407-4416. doi: [10.1007/s00330-020-06817-6](https://doi.org/10.1007/s00330-020-06817-6).
- 399 8. Li K, Wu J, Wu F, Guo D, Chen L, Fang Z, et al. The clinical and chest CT features
400 associated with severe and critical COVID-19 pneumonia. *Invest Radiol.* 2020;55:
401 327-331. doi: [10.1097/RLI.0000000000000672](https://doi.org/10.1097/RLI.0000000000000672).
- 402 9. Francone M, Iafrate F, Masci GM, Coco S, Cilia F, Manganaro L, et al. Chest CT score in
403 COVID-19 patients: correlation with disease severity and short-term
404 prognosis. *Eur Radiol.* 2020;30: 6808-6817. doi: [10.1007/s00330-020-07033-y](https://doi.org/10.1007/s00330-020-07033-y).
- 405 10. Liang T, Liu Z, Wu CC, Jin C, Zhao H, Wang Y, et al. Evolution of CT findings in
406 patients with mild COVID-19 pneumonia. *Eur Radiol.* 2020;30: 4865-4873. doi:
407 [10.1007/s00330-020-06823-8](https://doi.org/10.1007/s00330-020-06823-8).
- 408 11. Inoue A, Takahashi H, Ibe T, Ishii H, Kurata Y, Ishizuka Y, et al. Comparison of
409 semiquantitative chest CT scoring systems to estimate severity in coronavirus disease
410 2019 (COVID-19) pneumonia. *Eur Radiol.* 2022;32: 3513-3524. doi:
411 [10.1007/s00330-021-08435-2](https://doi.org/10.1007/s00330-021-08435-2).
- 412 12. Timaran-Montenegro DE, Torres-Ramírez CA, Morales-Jaramillo LM, Mateo-Camacho
413 YS, Tapia-Rangel EA, Fuentes-Badillo KD, et al. Computed tomography-based lung
414 residual volume and mortality of patients with coronavirus disease-19 (COVID-19). *J*
415 *Thorac Imaging.* 2021;36: 65-72. doi: [10.1097/RTI.0000000000000572](https://doi.org/10.1097/RTI.0000000000000572).
- 416 13. Colombi D, Bodini FC, Petrini M, Maffi G, Morelli N, Milanese G, et al. Well-aerated
417 lung on admitting chest CT to predict adverse outcome in COVID-19
418 pneumonia. *Radiology.* 2020;296: E86-E96. doi: [10.1148/radiol.2020201433](https://doi.org/10.1148/radiol.2020201433).
- 419 14. Grassi R, Cappabianca S, Urraro F, Feragalli B, Montanelli A, Patelli G, et al. Chest CT
420 computerized aided quantification of pneumonia lesions in COVID-19 infection: A

- 421 comparison among three commercial software. *Int J Environ Res Public Health*.
422 2020;17: 6914. doi: [10.3390/ijerph17186914](https://doi.org/10.3390/ijerph17186914).
- 423 15. Granata V, Ianniello S, Fusco R, Urraro F, Pupo D, Magliocchetti S, et al. Quantitative
424 analysis of residual COVID-19 lung CT features: consistency among two commercial
425 software. *J Pers Med*. 2021;11: 1103. doi: [10.3390/jpm11111103](https://doi.org/10.3390/jpm11111103).
- 426 16. Kauczor HU, Heitmann K, Heussel CP, Marwede D, Uthmann T, Thelen M. Automatic
427 detection and quantification of ground-glass opacities on high-resolution CT using
428 multiple neural networks: comparison with a density mask. *AJR Am J Roentgenol*.
429 2000;175: 1329-1334. doi: [10.2214/ajr.175.5.1751329](https://doi.org/10.2214/ajr.175.5.1751329).
- 430 17. Okuma T, Hamamoto S, Maebayashi T, Taniguchi A, Hirakawa K, Matsushita S, et
431 al. Quantitative evaluation of COVID-19 pneumonia severity by CT pneumonia
432 analysis algorithm using deep learning technology and blood test results. *Jpn J Radiol*.
433 2021;39: 956-965. doi: [10.1007/s11604-021-01134-4](https://doi.org/10.1007/s11604-021-01134-4).
- 434 18. Durhan G, Ardalı Düzgün S, Başaran Demirkazık F, Irmak İ, İdilman İ, Gülsün Akpınar
435 M, et al. Visual and software-based quantitative chest CT assessment of COVID-19:
436 correlation with clinical findings. *Diagn Interv Radiol*. 2020;26: 557-564. doi:
437 [10.5152/dir.2020.20407](https://doi.org/10.5152/dir.2020.20407).
- 438 19. Huang L, Han R, Ai T, Yu P, Kang H, Tao Q, et al. Serial quantitative chest CT
439 assessment of COVID-19: A deep learning approach. *Radiol Cardiothorac Imaging*.
440 2020;2: e200075. doi: [10.1148/ryct.2020200075](https://doi.org/10.1148/ryct.2020200075).
- 441 20. Aoki R, Iwasawa T, Hagiwara E, Komatsu S, Utsunomiya D, Ogura T. Pulmonary
442 vascular enlargement and lesion extent on computed tomography are correlated with
443 COVID-19 disease severity. *Jpn J Radiol*. 2021;39: 451-458. doi:
444 [10.1007/s11604-020-01085-2](https://doi.org/10.1007/s11604-020-01085-2).

- 445 21. Li Z, Zhong Z, Li Y, Zhang T, Gao L, Jin D, et al. From community-acquired pneumonia
446 to COVID-19: a deep learning-based method for quantitative analysis of COVID-19 on
447 thick-section CT scans. *Eur Radiol.* 2020;30: 6828-6837. doi:
448 [10.1007/s00330-020-07042-x](https://doi.org/10.1007/s00330-020-07042-x).
- 449 22. Shi H, Han X, Jiang N, Cao Y, Alwalid O, Gu J, et al. Radiological findings from 81
450 patients with COVID-19 pneumonia in Wuhan, China: a descriptive
451 study. *Lancet Infect Dis.* 2020;20: 425-434. doi: [10.1016/S1473-3099\(20\)30086-4](https://doi.org/10.1016/S1473-3099(20)30086-4).
- 452 23. Kurashima K, Kagiya N, Ishiguro T, Kasuga K, Morimoto Y, Ozawa R, et
453 al. Predictors of severe COVID-19 pneumonia. *Kansenshogaku Zasshi.* 2020;94:
454 483-489. doi: [10.11150/kansenshogakuzasshi.94.483](https://doi.org/10.11150/kansenshogakuzasshi.94.483).

Fig. 1



	lung	LAV	LAV %	nLAV	nLAV%
total	4158.82cc	3822.92cc	91.92%	335.90cc	8.08%
left lung	1945.06cc	1757.83cc	90.37%	187.23cc	9.63%
LU	128.95cc	1012.16cc	89.68%	116.19cc	10.32%
LL	816.11cc	745.37cc	91.33%	70.74cc	8.67%
right lung	2213.76cc	2065.09cc	93.26%	148.66cc	6.72%
RU	525.88cc	487.86cc	92.75%	38.13cc	7.25%
RM	680.66cc	531.37cc	95.57%	29.29cc	4.43%
RL	1027.12cc	945.87cc	92.08%	81.25cc	7.91%

Histogram

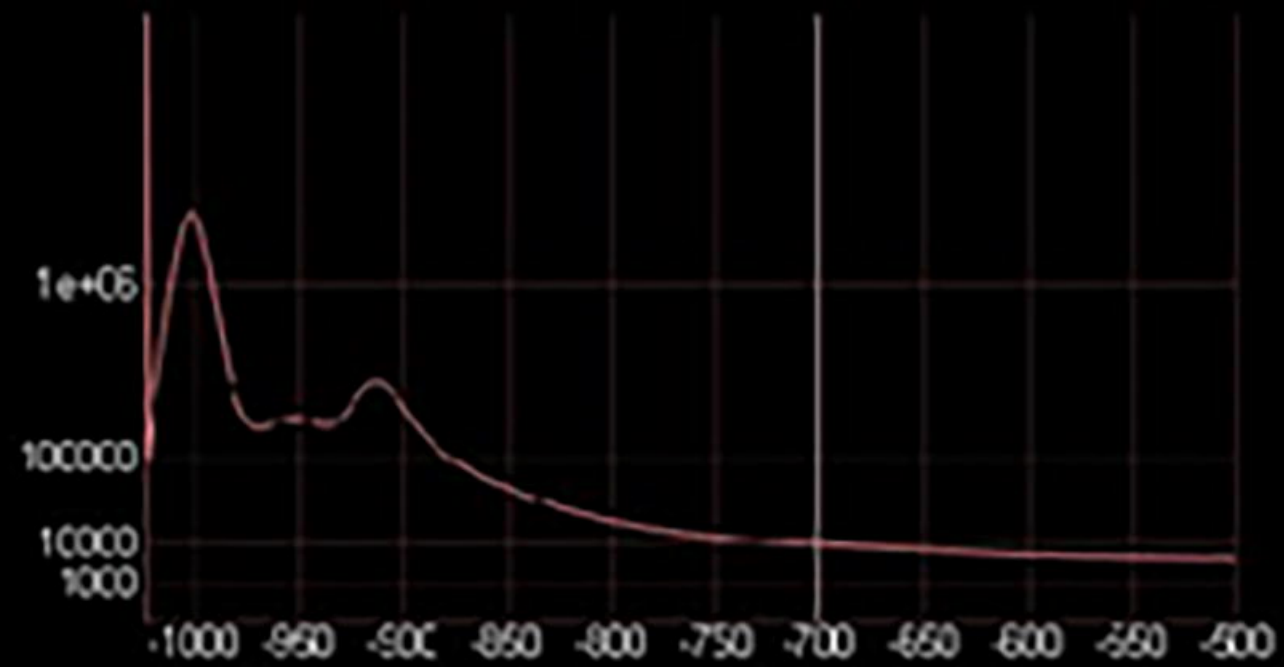


Fig. 2
: -884.00
: 899.00
: 184.83

area : 439.65 mm²
mean : -657.44
min : -906.00
max : -119.00
SD : 148.78

: 598.28
: -579.6
: -871.0
: 29.00
: 168.63

: 14873.18 mm²
: -554.32
: -945.00
: 899.00
: 229.06

: 12730.09 mm²
: -766.13
: -940.00
: 638.00
: 157.41



Fig. 3

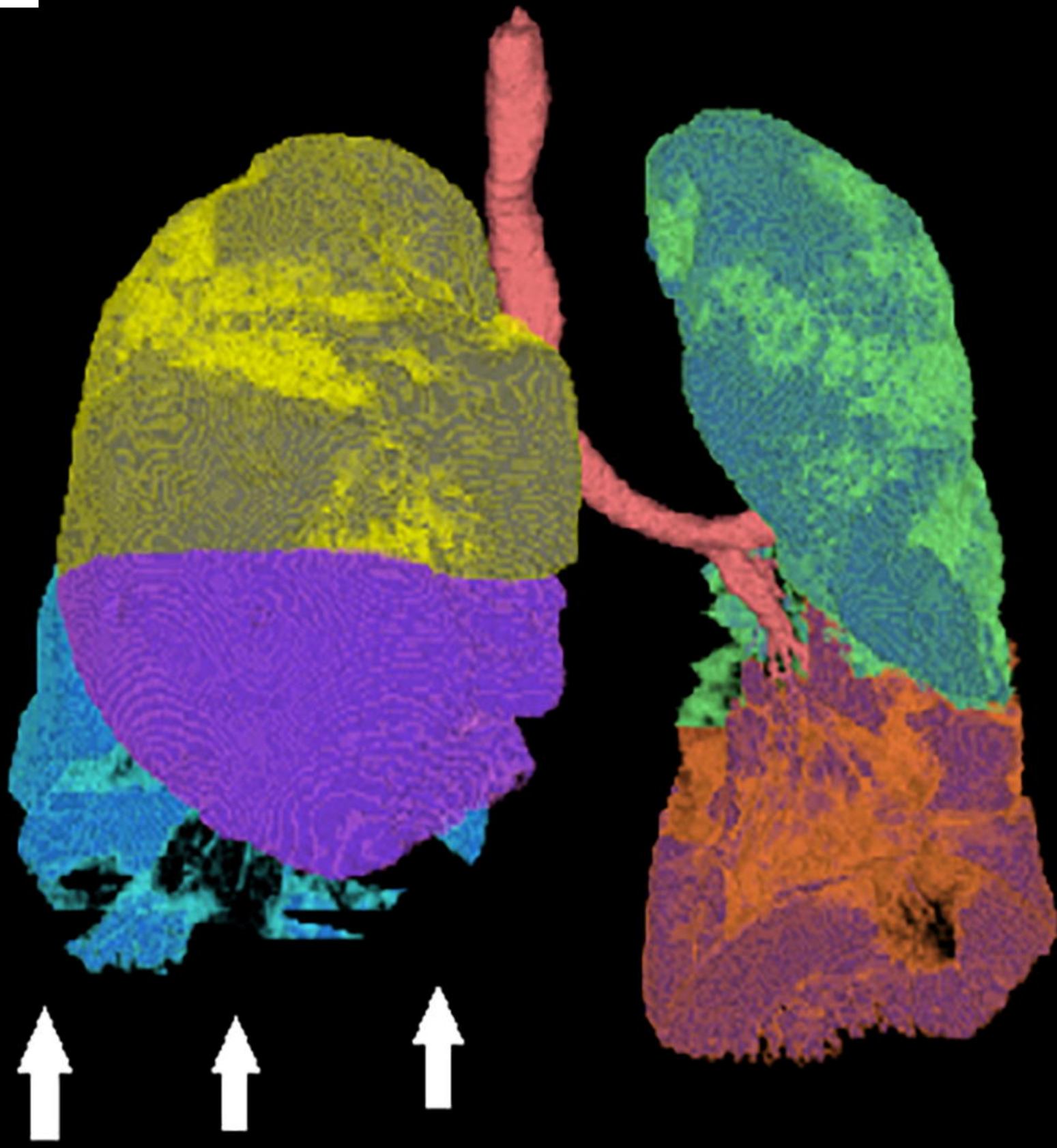
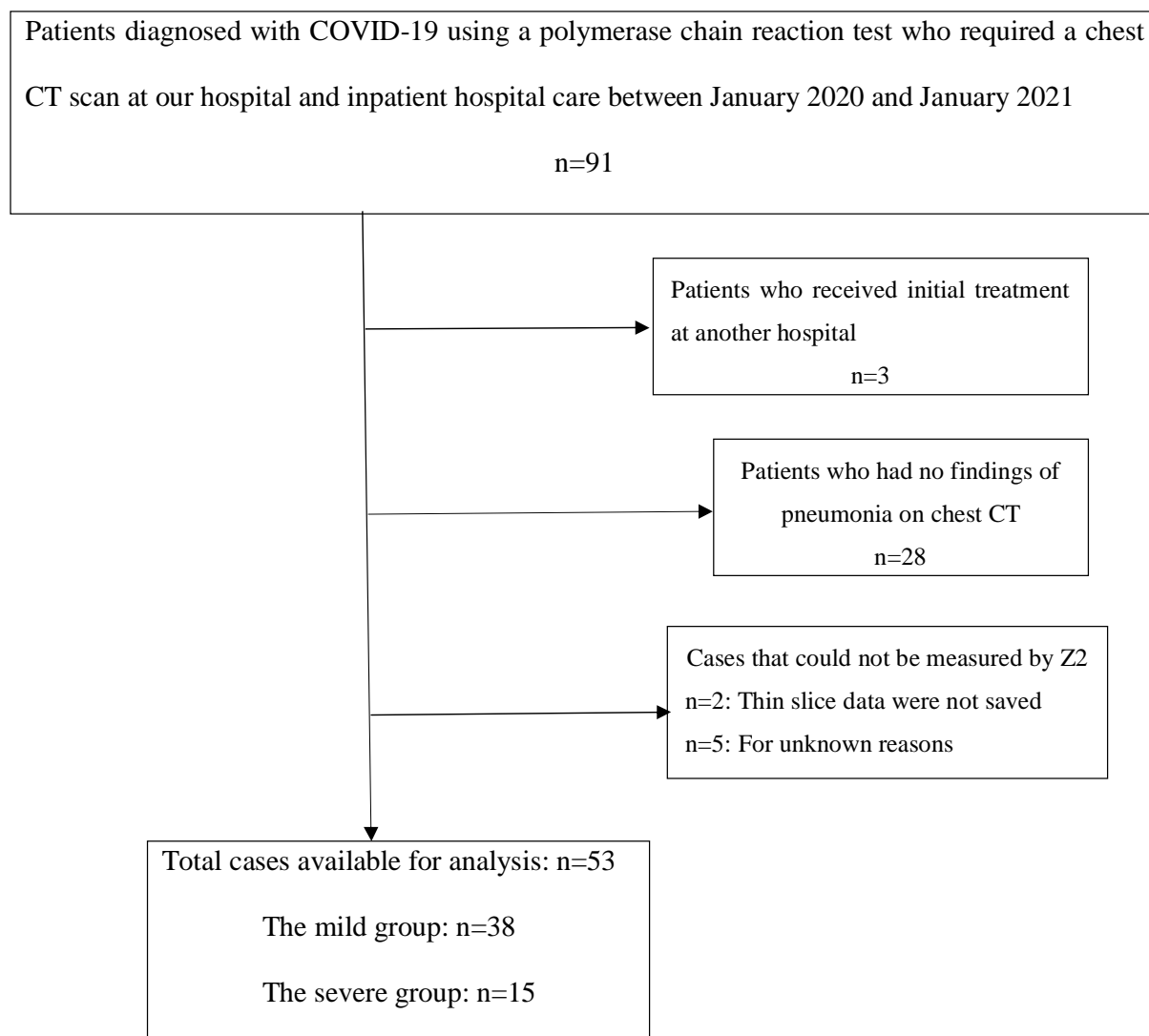


Fig 4.



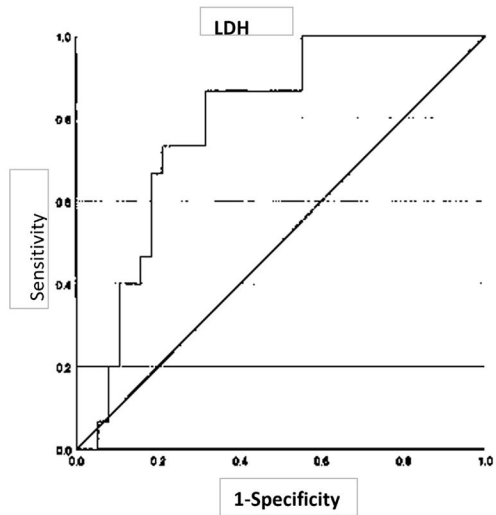
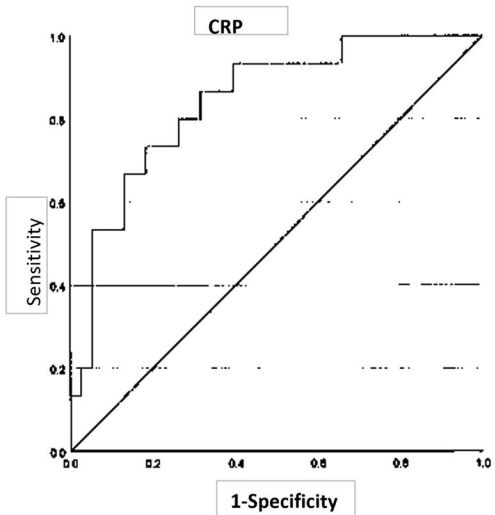
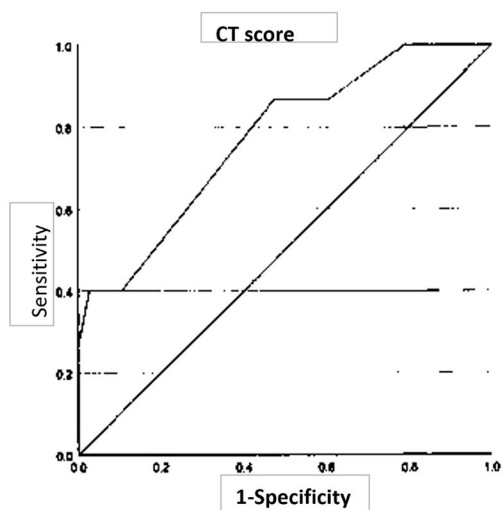
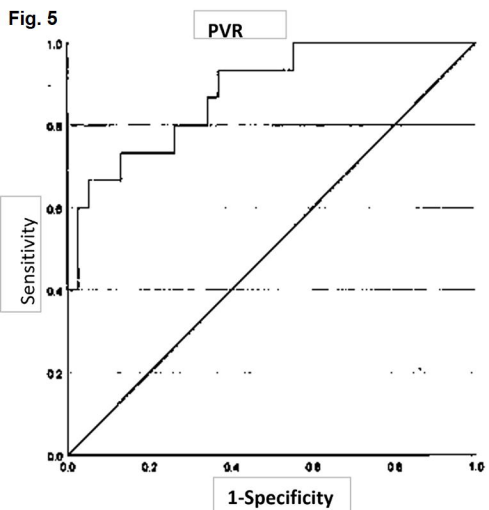


Fig. 6

